International Journal of Geomagnetism and Aeronomy
Vol 2, No. 2, August 2000

# APEX: Experiments with neutral xenon releases

*V. N. Oraevsky, V. S. Dokukin, A. S. Volokitin, S. A. Pulinets, and Yu. Ya. Ruzhin*

**Institute of Terrestrial Magnetism, Ionosphere, and Radio Wave Propagation, Troitsk, Moscow Region, Russia**

*E. Chouieri*

**Electric Propulsion and Plasma Dynamics Laboratory, Princeton University, New Jersey, Princeton, USA**

*V. V. Afonin*

**Institute of Space Research, Moscow, Russia**

### Contents



## Abstract

Observations of broadband HF wave spectra and parameters of cold plasma obtained at injection of a jet of neutral xenon in the ionosphere in the course of the Active Plasma Experiment (APEX) project are presented. The theoretical models for the influence of gas injection on the ambient plasma and observed effects related to the abnormal ionization phenomenon are discussed.

## 1. Introduction

The phenomenon of critical ionization velocity (CIV) is a fast (abnormal) ionization of a neutral gas occurring when the relative speed of a gas cloud in a magnetized plasma exceeds some critical value at which the atom kinetic energy is higher than its ionization potential. This fundamental phenomenon of plasma physics was proposed by *Alfvén* [1954] as an explanation of various aspects of the formation of the solar system and ionospheres of both distant planets and comets. The CIV phenomenon includes, as an essential component, the development of low-frequency plasma turbulence due to interaction of the ion beam with the plasma waves. The wave-particle and nonlinear

wave-wave interactions, characteristic for this low-frequency turbulence, provide heating and acceleration of electrons and, as result, ionization of the neutral gas [*Haerendel*, 1982; *Papadopoulos*, 1985].

The CIV phenomenon was a goal of many theoretical [*Galeev and Chabibrachmanov*, 1986] and experimental [*Torbert,* 1990] investigations over the last few years. An opportunity to use the Earth's ionosphere and magnetosphere as an ideal laboratory for the experimental study of the CIV phenomenon is attractive, and a number of active experiments in space with injection of neutral gas has been carried out: Porcupine [*Torbert*, 1990], Condor [*Haerendel et al.,* 1986], Star of Lima [*Wescott et al.*, 1986], the ATLAS 1 [*Marshall et al.,* 1993]. The observations of a low-frequency turbulence excited in a magnetized plasma by an ion beam or plasma jet, obtained in the COMBI and Porcupine rocket experiments, are of interest also for studying the CIV phenomenon, as a basic process, controlling ionization of a neutral gas cloud. Unfortunately, many CIV details in these experiments still remain obscure and even a manifestation of the CIV in some of them remains doubtful.

Conducting the experiments with injection of xenon plasma (beams of Xe ions) in the ionosphere in the scope of the APEX (Active Plasma Experiment, which was an Institute of Terrestrial Magnetism, Ionosphere, and Radio Wave Propagation (IZMIRAN) project) program, there were more than 20 cases not planned beforehand, when the plasma gun operated in a mode of neutral gas injection. Under the conditions of the APEX the kinetic energy of the relative movement of Xe atoms and the ionospheric plasma exceeded the xenon ionization potential, so the obligatory condition of the CIV phenomenon was fulfilled. The injections of neutral xenon were made in a height range from 400 up to 3000 km. The experimental conditions (the values of the geomagnetic field, background density, angle between the vector of the gas velocity and the magnetic field, etc.) considerably changed along the polar orbit of the spacecraft, and this is a distinctive feature of the experiment as compared with other experiments, for example, ATLAS 1.

Since the research of anomalous ionization was not part of the original APEX program, the satellite was not designed with an ability to increase the neutral xenon mass flow above the nominal value of 3 mg $s^{-1}$. This is 3 orders of magnitude lower than the gas output in the ATLAS 1 experiment. However, contrary to the gas injections at ATLAS 1, which lasted 100 ms each, the duration of the gas releases in APEX was a few minutes.

Analyzing the APEX data for the processes responsible for CIV, one should investigate the following: influence of the gas injection on the electron distribution and the spectra of low-frequency plasma waves, dependence of the plasma turbulence spectra on the angle between the magnetic field and the gas motion direction, and other effects. The observations of the xenon ions with the characteristic energy corresponding to the kinetic energy of the atoms, the spectra of accelerated electrons, and electric field oscillations in the vicinity of the lower hybrid resonance also are of interest.

The data obtained in the experiment indicate that the ambient plasma reacted to the impact of the neutral gas flow. In some cases, changes in the density, temperature and plasma anisotropy, variations of the spacecraft potential, and an increase of the wave activity almost in the entire frequency range are observed.

The structure of the paper is as follows: Section 2 describes briefly the satellite instrumentation. Section 3 discusses the experimental data based mainly on the onboard observations of the cold plasma and HF waves. A theoretical analysis of the interaction of the neutral cloud with the plasma in the APEX is presented in section 4. The analysis includes consideration of the processes of the gas preionization and formation of a nonequilibrium distribution of the ions, quasi-linear theory of instability of a spatially limited ion beam in the plasma, including electron heating in this process, and also discussion of extra ionization of the neutral gas and other effects accompanying CIV. Section 5 contains the results of the above analysis.

## 2. General Description of the Diagnostic Equipment and Regimes of Neutral Xe Injection in the APEX Project

The scientific equipment onboard the Intercosmos 25 spacecraft includes two electron guns with the acceleration voltage of 8 keV and a current of 100 mA, the injector of neutral gas and Xe plasma with the effective current of 2-4 A, and also the scientific devices, which provide measurements of microparameters and macroparameters of the thermal and "suprathermal" plasma components, quasi-constant components of the magnetic and electric fields, and electromagnetic fields in the ELF/VLF/LF/HF ranges. The devices, whose measurements are of interest in studying anomalous ionization, are briefly described below.

The HF wave block provided measurements of one component of the electric and magnetic field in the frequency range 0.1-10 MHz. The data are discussed below.

The ionospheric plasma parameters (the ion density and three components of the electron temperature) were measured by the KM-10 device, which uses flat nickel probes with a diameter of 3.5 cm as sensors. One of the probes was chosen for permanent control of the probe potential relative to the spacecraft body. Due to a high input impedance of the differential amplifier, the probe potential was close to the one given by the balance between the electron flux and the flux of the inflowing ions. The KM-10 device was able to measure the potential residual up to $\pm$ 90 V, this value being limited by the amplifier. The detector part of the device was fixed at the rod and installed at a distance of 1 m in front of the solar panels in the direction of the spacecraft velocity.

The quasi-constant magnetic field was measured by the three-axis magnetometer with a dynamical regime of $\pm$ 64,000 nT. The data of the other (service) three-axis magnetometer, which was a part of the navigation system, were also available.

Xenon injection was conducted through a stationary plasma injector (UPM), which operated in the regime without discharge ignition. The plasma injector was put into the upper part of the spacecraft with its axis directed under an angle of $45^o$ to the spacecraft vertical axis. Due to some technical reasons, the ionization voltage was not switched on in 20 operational series. The standard regimes of the UPM operation contained a 5 to 6 s interval with a release of xenon neutral atoms in the beginning of each session. The kinetic energy of the xenon atom relative motion was above 20 eV and exceeded significantly the xenon ionization potential $U_I$ = 12.13 eV; however, the total mass of the injected xenon atoms was relatively small, and so one should hardly expect observation of all the manifestations of the anomalous ionization process (a total CIV) in these experiments. Nevertheless, some physical processes participating in CIV may be observed.

## 3. Observations

The only distinct manifestation of effects of the neutral gas injection in the observational data analyzed up to date is in the results of the wideband measurements of HF waves in the MHz range. Most probably, this result of the search for manifestation of the anomalous ionization processes may be due to the low flux density (small mass) of the gas injected in the APEX experiment. Even if the conditions of ion beam instability were realized, the turbulence developed was much weaker than that registered in the ATLAS 1 experiment [*Marshall et al.*, 1993].

The HF wave activity observations are represented by the following broadband data, which demonstrate two cases of injection with high and low pitch angles and manifest distinctly strong pitch-angle dependence. The observed effects may be summarized as follows:

In all neutral xenon releases studied with a high (close to the normal) pitch angle (between $85^o$ and $115^o$) an intensification of the emission of the HF plasma waves in the frequency range 3-10 MHz is observed.

In all releases with low pitch angle (between $57^o$ and $71^o$) studied, no such intensification of the wave emission was observed.

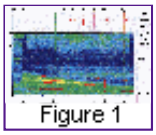
Figure 1

Figure 1 shows typical broadband HF spectra in the range 1-10 MHz for the neutral xenon injection at orbit 419 (the orbit parameters are shown in Table 1). The signal amplitude is shown by the color, the injection moments are shown by vertical lines. The red curves show the first three harmonics of the electron cyclotron frequency. The injection was conducted with a high pitch angle, beginning from $94.8^o$ at valve opening moment and ending at $113^o$ at closing.

Figure 1 shows the following features of the broadband spectra:

1. There is wave activity in a narrow band (manifested as a light blue band with some green in it) with a center at approximately 3.7 MHz, which begins at the valve switching on (with the accuracy up to the device resolution) and continues till the valve is switched off.

2. There is more wideband activity, mainly manifested as a green band with some blue colors spread from 8 MHz up to a frequency of at least 10 MHz. This wave activity has the same properties as the above described narrowband activity, except that the emission stops more abruptly when the valve is switched off.

3. Both of the above described wave bands are horizontal and do not manifest temporal changes in the magnetic field, which would cause variations in the electron-cyclotron frequency harmonics shown in Figure 1.

4. All other properties are either natural ionospheric phenomena or wave activity, which is not influenced by the neutral gas release.

Complete explanation of the character of this wave activity is a hard task. Since the frequencies of the amplified waves do not manifest significant changes in the magnetic field and density during the data registration time, they cannot be directly related to the natural plasma frequencies. Nevertheless, the fact stays that their appearance and properties observed correspond well to the gas release events.

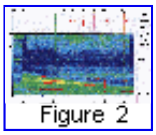
Figure 2

Another example of the broadband HF data for a release with high pitch angle is shown in Figure 2. The injection took place at orbit 490 with the parameters shown in Table 1. The same comments are true here as have been done for Figure 1 (for orbit 419) with some addition that there is a distinct increase of the broadband noise over the entire spectrum. The increase starts from the moment of the switching on the cathode heater and stops at the moment of switching off all UPM subsystems.

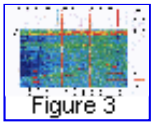
Figure 3

An example of the injection with low pitch angle is shown in Figure 3 for orbit 496. The corresponding orbital data are also shown in Table 1.

Contrary to the high-angle injection discussed above, these data show no change in the wave activity, which might have been related to any event of the neutral gas release.

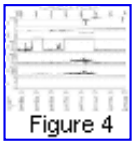
Figure 4

The results of the measurements of the cold plasma parameters in the periods of neutral gas injection show no significant changes in the plasma density. Figure 4 shows the results of the measurements of the plasma density and temperature and the spacecraft potential by the KM-10 device at orbit 419. These data have been filtered to exclude telemetry noise and

demonstrate rather strong variations of the plasma density and temperature and also of the spacecraft potential not related to the xenon injection.

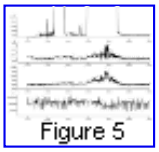
Figure 5

The variations of the plasma density and electron temperature along and across the magnetic field are shown in Figure 5 versus the number of the telemetry frame, which corresponds to a time dependence. In spite of the fact that a strong noise related to telemetry fails is seen in Figure 5, the character of the ρ and $T_e$ changes is fairly distinct, and one can conclude that there is no significant changes in the density related to the gas injection. There is a small peak at the temperature dependence, which coincides with the time of gas injection, but it is, most probably, an effect of the heating or acceleration of the electrons under the interaction of the xenon jet with the ambient plasma.

It should be emphasized that though the above described effects correlate well with the pitch angle in all the cases considered, it is still obscure, whether this correlation is of a random character or whether the appearance of the above mentioned emissions is governed by other conditions, for example, by the position at the orbit and plasma parameters which correlate with the pitch angle.

In particular, it is interesting that all the high pitch-angle injections studied were carried out under solar illumination, whereas all the small pitch-angle injections were conducted in darkness. This fact is a consequence of the unplanned synchronism between the motion along the polar orbit, solar illumination cycle and injection program. Therefore it is possible that the presence of the sunlight fluxes, but not the pitch angle value, is the governing parameter for the effects described above. In this case the role of the solar flux, in excitation of the broadband HF activity by the effects of the type of plasma expansion due to the photoionization, is worth studying. Since the changes in the sunlight flux during the injection time are small and the gas expenditure under the injection is constant, such a mechanism may provide explanation to the constancy of the excited band frequency with time.

In conclusion, we cannot exclude the role of ground-based radio sources in formation of the horizontal frequency bands observed in the spectra. However, the question still remains, why these bands appear (or are intensified) only during injections.

---

## 4. Theoretical Model

The gas expenditure in the regime of neutral gas injection corresponds to the injection plasma current (2-3 A) of $dN_{Xe}/dt$ = 2-6 × $10^{19}$ atoms per second. The mean release velocity $v$ is 1-2 $v_T$ ( $v_T$ being the Xe thermal velocity in the reservoir). Though the value of $v_T$ is not exactly known, one can accept that $v_T \leq 10^4$ cm s $^{-1}$. As a result, a neutral gas cloud, which moves with a velocity of 5 ± 8 km s $^{-1}$ through the ambient plasma, is formed around the spacecraft. We assume that the cloud forms a spherical cone with the angle of $60^o$ and a ring in the lateral cross section. Assuming that the gas density in the spherical cone is homogeneous within the cross section (to be more exact, one can assume a Gaussian distribution of the density), one can express it at a distance $r$ as

$$n_{Xe} = \frac{dN_{Xe}}{dt}\frac{1}{2\pi r^2 v_T} = \frac{10^{15}}{r^2} \qquad (1)$$

Here $d N_{Xe} / dt$ = (2-6)× $10^{19}$ atoms per second and the velocity $v = v_T \leq 10^4$ cm s $^{-1}$. For example, at $r$ = 100 m and 1000 m, $n_{Xe} = 10^9$ cm $^{-3}$ and $10^7$ cm $^{-3}$, respectively.

If some of these Xe atoms are ionized, the interaction of these ions with the ambient plasma may initiate a process of anomalous ionization. There are several possibilities to reach the necessary

preionization. They are as follows: ionization by electric charges in the injector, Xe atom ionization in inelastic collisions with the ions of the ambient plasma with charge transfer, electron impact ionization in collisions with the plasma electrons, and photoionization. We assume that at least in 20 cases of neutral gas release, the first possibility should be excluded. So we consider the efficiency of the latter three processes.

### 4.1. Xe Ionization Under Collisions With Charge Transfer

Inelastic collisions of the Xe atoms with $O^+$ ions with a charge transfer have the cross section $\sigma_{ch} \approx 2 \times 10^{-15}$ cm $^2$, which is lower than the elastic collision cross section. The local formation rate of the Xe ions in the charge transfer reaction may be evaluated as

$$d\, n_{Xe^+} = \langle \sigma_{ch}\, n_i v \rangle \; n_{Xe}$$

Bearing in mind that the number of the atoms injected increases linearly with time, we obtain, after integration over the volume, the total number of the Xe ions formed during time $t$ in charge transfer collisions with plasma ions

$$\bar{N}_{Xe+} = t \int \langle \sigma_{ch}\, n_i v \rangle n_{Xe}\, dV$$

$$= \langle \sigma_{ch}\, n_i v \rangle t \int^{r/v_T} \frac{dN_{Xe}}{dt} \frac{d^3 r}{r^2 v_T} \approx \langle \sigma_{ch}\, n_i v \rangle t \frac{dN_{Xe}}{dt} \frac{r}{v_T}$$

$$\sim \langle \sigma_{ch}\, n_i v \rangle \frac{dN_{Xe}}{dt} t^2 \approx 10^{15} t^2$$

One can hardly expect an ability to observe the newly born ions by the diagnostics available at the spacecraft. First of all, the Larmor radius of the Xe ions is high ( $r_L \geq$ 500 m). Then, the Xe ions never reach the spacecraft (the diagnostic tools) because of both, [ $\mathbf{E} \times \mathbf{B}$ ] drift and the initial velocities.

### 4.2. Impact Ionization by Plasma Electrons

The evaluation of the number of the Xe ions formed in inelastic collisions with the plasma electrons may be done in the same way as it has been done in the previous section. However, a significant difference should be taken into account. Under the ambient plasma electron temperature of 1-2 eV, the number of the electrons with the energy exceeding the ionization potential is very low. Therefore the effective ionization frequency

$$\langle \sigma_{e\,\mathrm{ion}} n_e v \rangle \approx 10^{-16}\, n_e\, v_{Te}\, e^{-eU_i/Te}$$

and the local ion formation rate may be evaluated by

$$d\, n_{Xe^+} = \langle \sigma_{e\,\mathrm{ion}} n_e v \rangle \; n_{Xe} \approx 10^{-16}\, n_e\, v_{Te}\, e^{-eU_i/Te}\, n_{Xe}$$

Now we obtain the evaluation of the total Xe ion formation under the electron impact ionization

$$\bar{N}_{Xe^+} = t \int \langle \sigma_{eion} n_e v \rangle n_{Xe} dV$$

$$\approx \langle \sigma_{eion} n_e v \rangle t \frac{dN_{Xe}}{dt} \frac{r}{v_T}$$

$$\sim 10^{-16} n_e v_{Te} e^{-eU_i/T_e} \frac{dN_{Xe}}{dt} t^2 \approx 10^{13} t^2 \qquad (2)$$

and see that the ionization rate in the charge transfer reaction is higher by 2 orders of magnitude.

The consequences of the Xe ion appearance in the environment under neutral gas injection are discussed below. However, there is another process, not considered above, which is a more effective source of plasma disturbance, leads to a heating of the ambient plasma, and creates prerequisites to anomalous ionization. The process is the reflection of the ambient plasma ions under elastic collisions with the neutral gas jet, which we consider in section 4.3.

### 4.3. Elastic Reflection of Ambient Plasma Ions in Collision With the Neutral Xe Jet

The gas density in the vicinity of the injector is high, and collisions of the Xe atoms with the ambient ions may be significant. We evaluate the distance from the injector at which the mean free path of the ions in the neutral gas $\lambda = 1/\sigma n_{Xe}$ is less than or equal to this distance ( $r_c = \lambda$ ). If the elastic collision cross section $\sigma$ is $10^{-14}$ cm $^2$, at the distance of less than 10-20 cm from the injector, actually the entire flux of the ionospheric plasma through the very beginning of the Xe cloud would be stopped (or reflected and scattered) due to collisions with the neutrals.

The inelastic collisions are able to influence the distribution function up to a distance of 100-300 cm. The probability of an ionospheric ion to be scattered in the Xe cloud at the path *dl* is about *dl*/$\lambda$. Then passing the path *dl* through the cross section *dS* in the Xe cloud, the ionospheric ion flux of about $\langle n_i v \rangle$ loses

$$d\bar{N}_i = \langle n_i v \rangle dS \frac{dl}{\lambda} = \langle n_i v \rangle \sigma n_{Xe} dS dl$$

particles per second. The total number of the ionospheric ions reflected per second is given by

$$\bar{N}_i = \langle n_i v \rangle \int \sigma n_{Xe} dS dl$$

$$= \langle n_i v \rangle \sigma n_{Xe} dV = \langle n_i v \rangle \sigma N_{Xe}$$

where $N_{Xe}$ is the total number of the injected Xe atoms. Thus under typical parameters ( $n_i \approx 10^4$, $v \approx v_{sc} \approx 8 \times 10^6$ cm s $^{-1}$ ) after *t* seconds the total flux of the scattered $O^+$ ions is

$$\bar{N}_i = \langle n_i v \rangle \sigma \frac{dN_{Xe}}{dt} t \approx (10^{15} - 10^{16}) t \qquad (3)$$

The oxygen ion energy almost do not change after a collision because of the large difference between the $O^+$ and the Xe masses. So as a first approximation, the reflected ion distribution may be considered as isotropic in the frame of reference of the Xe cloud (spacecraft). The ionospheric ions

reflected from the neutral cloud are magnetized and continue the [ **E**× **B** ] drift in the cloud system together with the main flux. However, in the frame of reference of the ionospheric plasma at a distance shorter than the Larmor radius, the reflected ions or a hot ion flux with the drift velocities about $v_{sc}$ and the velocity scatter within about (1/2-1/3)$v_{sc}$.

Thus some part of the ionospheric ion flux is captured by the neutral Xe cloud. This effect of raking together may be observed and the ionospheric plasma ion density may increase. However, the main effect of the ion collisions with the Xe gas is formation of an unstable (beam) velocity distribution and, as a result, generation of the lower hybrid oscillations in the plasma. The ion flux formed is significantly irregular in space. We are able to evaluate the flux density, which is a principal parameter controlling the instability conditions, if we assume that the distance $R$ (the main input to the flux density) is provided by the ions scattered for $r < R$ and $t \approx R/v_T$. Thus

$$\frac{n_b}{n_i} = \frac{\bar{N}_i}{n_i v_{sc} R^2} = \frac{\langle n_i v \rangle}{n_i v_{sc}} \frac{\sigma dN_{Xe}}{v_T R^2 dt} R = \frac{\sigma dN_{Xe}}{v_T R dt} = \frac{60}{R}$$

For $R \leq 10^4$ cm we obtain $n_b n_i \sim 10^{-3}$-$10^{-4}$.

### 4.4. Electron Heating

Acceleration or heating of the electrons by waves under development of the ion-ion instability is usually considered as a significant part in the chain of events leading to anomalous ionization in the rarefied medium. Evaluation of the typical mean free path of the ionospheric electrons in the Xe cloud under elastic collisions ( $\sigma_{e\text{-}Xe} \sim (0.3\text{-}1) \times 10^{-15}$ cm $^2$ ) and neutral density ρ is given by

$$\lambda_{e-Xe} \approx \frac{1}{n_{Xe} \sigma_{e-Xe}} \approx (1 - 3) r^2$$

Here $r$ is the distance from the injector in meters. This formula shows that the $e$ -Xe elastic collisions are significant up to $r \sim 1$ m. At distances $r > 3$ m, electron collisions occur very seldom to change their dynamics or distribution. According to the previous consideration, the density of the plasma ions scattered by the Xe atoms is rather high at $r \leq 3$ m, and in this region, oscillations of the ion sound type may develop, leading to a strong heating of the electrons (this is possible under their capture and crossing of trajectories in the wave potential). The energy of the accelerated electrons may be evaluated, if we assume that the ion-ion instability is stabilized by the ion trapping in the potential hole $\varphi_{trapp}$. In this case the electron obtains additional energy $\varepsilon \sim e\varphi_{trapp} = m_i v dv = 3 \pm 5$ eV, where $dv$ is the velocity shift between the beam and the wave. Thus the heating of the electron to energies higher than the ionization potential is possible only in resonance interaction with waves of much longer wavelength in a much larger volume.

Thus the reflected ions form a bump-of-tail distribution near the injector. In this case, development of ion-ion instability is possible, because the relative velocity $V_b$ of the ionospheric plasma and the ions of the beam exceeds significantly the thermal velocity of the background plasma ions. The ion-sound instability is suppressed in the ionosphere under $T_e \approx T_i$, and under these conditions, the main instability is the instability of the quasi-potential lower hybrid oscillations under their resonance interaction with the ion beam $kV_b \approx -k_\perp | V_b | \approx \omega = \omega_c(k_z/k)$, where $\omega_{pe}$ and $\omega_c$ are Langmuir and electron cyclotron frequencies, respectively. It is assumed that $\omega \ll \omega_c$, and the parallel vector of the wave $k_z$ is less than the $k_\perp$ vector perpendicular to the magnetic field. Taking the wavelength of the instable wave to be less than the ion cloud dimension, we calculate the local instability increment of the ion beam according to [*Mikhailovskii,* 1974]

$$\gamma_b = \omega \frac{\omega_{pi}^2}{1 + (\omega_p / \omega_c)^2} \left( \frac{1}{k \Delta V_b} \right)^2 \left( \frac{n_b}{n_i} \right) \sim \omega \left( \frac{n_b}{n_i} \right) \geq 10^2$$

where $\Delta V_b$ is the velocity dispersion in the beam, which in our case is about $1/2 V_b$.

The threshold of the ion-ion instability is determined by the velocity, with which the wave exits the region of the interaction with the beam. The velocity may be represented by the effective attenuation rate $\nu = V_{gz}/R$, where $V_{gz}$ is the group velocity of the waves $V_{gz} = \partial \omega / \partial k_z = \omega / k_z$. The necessary condition $\gamma_b \geq \nu$ is fulfilled if $k_z R \geq n_i n_b \approx 10^3$.

Above the threshold the instability is saturated because of the quasi-linear resonance interaction of electrons with the lower hybrid waves. If the equilibrium state is reached and there is a balance of the swinging and attenuation rates of the waves according to the equation

$$(\gamma_b + \gamma_e) W_k = 0$$

one is able to determine the distribution function of the electrons accelerated as a result of development of the ion beam instability. Here $W_k$ is the wave energy density, $\gamma_e$ is the Landau damping under the resonance $\omega = k_z v_{ez}$ with the magnetized electrons, which is given by the formula

$$\gamma_e = \omega \frac{\omega_{pe}^2}{k^2 (1 + (\omega_{pe} / \omega_c)^2)} \frac{\partial F_e}{\partial v_{ez}} \Bigg|_{v_z k_z = \omega}$$

Using the equation

$$\frac{\partial F_e}{\partial v_{ez}} = -\frac{\gamma_b}{\omega} \frac{k_z^2 (1 + (\omega_{pe} / \omega_e^2))}{\omega_{pe}} \simeq -\left( \frac{m_e}{m_i} \right) \frac{1}{\Delta V^2} \frac{N_p}{N_{Xe}} \qquad (4)$$

we find a solution [see *Lizunov et al.*, 1995], which is a universal distribution of the accelerated electrons:

$$F_e(v_z) = 2 \frac{n_{supra}}{n_0} \frac{v_{max} - v_z}{v_{max}^2}$$

where

$$\frac{n_{supra}}{n_0} = \left( \frac{m_e}{m_i} \right) \frac{v_{max}^2}{\Delta V^2} \frac{N_p}{2 N_{Xe}}$$

The maximum velocity, to which the waves may accelerate the electrons, is determined by the condition

$$v_{max}^2 = D_{zz} \tau = D_{zz} L_{||} / v_{max} \qquad (5)$$

where

$$D_{zz} = \omega_{pe}^2 \int \left( \frac{k_z}{k_\perp} \right)^2 \frac{E_k^2}{4 \pi n m_e} \delta(\omega - k_z v_{ez}) d k_z d(\pi k_\perp^2)$$

is the coefficient of the electron diffusion in the velocity space. Further we use the expression

$$D_{zz} = v_{Te}^2 \omega_{pe}^2 \frac{W_k}{nT_e} \frac{k_z^2}{v_z k_\perp^2} = v_{Te}^2 \omega_{pe}^2 \frac{W_k}{nT_e} \left(\frac{\omega}{\omega_e}\right)^2 \frac{k}{\omega}$$

where

$$W_k = \int (E_k^2/4\pi) d(\pi k_\perp^2)$$

is the energy distribution along the spectral lines, and the $k_\perp = k_\perp(k_z)$ ratio is taken along this line. Taking into account the resonance condition $\omega/k \simeq V_b$, we can estimate

$$D_{zz} = \omega_* v_{Te}^2 \frac{\omega_{pe}^2}{2\omega_e^2} \frac{W}{nT_e}$$

where

$$W = \int W_k dk_z$$

and $\omega_*$ is the frequency, corresponding to maximum of the spectrum. Then from (4) and (5)

$$\frac{v_{max}^3}{v_{Te}^3} \simeq \frac{\omega_*}{\omega_e} \frac{L_{||}}{\rho_e} \frac{\omega_{pe}^2}{\omega_e^2} \frac{W}{nT_e}$$

Unfortunately, the quasi-linear theory is not able to determine $W/nT_e$ and $\omega_*$ with reasonable accuracy. To be able to accelerate electron to energy exceeding the potential ionization ($v_{max}^2 / v_{Te}^2 \geq 30$), one has to reach (at $\omega_{pe}^2/\omega_e^2 = 10$ and $\omega_* \simeq 10^{-2}\omega_e$)

$$\frac{L_{||}}{\rho_e} \frac{W}{nT_e} \geq 3 \times 10^3$$

This condition is rather difficult but possible to satisfy at realistic $W/T_e = 3 \times 10^{-2}$ and $L_| = 10^5 \rho_e$.

### 4.5. Ionization of Xe by Accelerated Electrons

The suprathermal electrons accelerated by the lower hybrid turbulence provide an extra source of ionization of Xe. The rate may be evaluated if one uses the calculated electron distribution in the same way as in section 4.2

$$\frac{dN_{Xe}^+}{dt} \int \sigma_{eion}(v) Fe(v) dv \int n_{Xe} dV \approx \langle \sigma_{eion} n_e v \rangle N_{Xe}$$

$$\frac{1}{t_{ion}} = \frac{d \log N_{Xe+}}{dt} \sim \frac{1}{3} \sigma_{eion}(v_{max}) n_{supra} v_{max}$$

$$\approx 6 \times 10^{-16} n_0 \left(\frac{m_e}{m_i}\right) \frac{v_{max}^3}{\Delta V^2} \frac{N_p}{6N_{Xe}}$$

$$\approx 10^{-16} v_{max} n_0 \frac{m_e}{m_i} \frac{v_{max}^2}{m_i \Delta V^2} \frac{N_p}{N_{Xe}} \approx 10^5$$

Here

$$\frac{m_e}{m_i} \frac{v_{max}^2}{\Delta V^2} \approx 0.3 - 1, \quad N_p / N_{Xe} \approx 10^{-2}.$$

For example, only 1% of the atoms would be ionized during the neutral Xe injection time of about 1000 s.

---

## 5. Conclusion

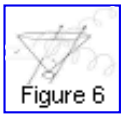
Figure 6

It follows from our theoretical consideration that (1) the amount of the injected neutral Xe is small. However, due to the collisional interaction of this gas with the background plasma, there appear enough initiating ions. They are new Xe ions and the scattered ions of the ionospheric plasma. (2) One may expect development of the ion-ion instability of the lower hybrid waves at a distance of $r \sim$ 3-100 m. These waves in the satellite frame of reference are perpendicular to the magnetic field component of the phase velocity in the range of the reflected ion velocities of 0-7 km $s^{-1}$. Their group velocity is directed mainly along the magnetic field, so they are able to reach the spacecraft and be observed. (3) In a quasi-linear interaction the lower hybrid wave accelerates the electrons along the magnetic field up to suprathermal energies. These electrons may reach the spacecraft and be observed (see Figure 6). (4) The expected flux of these electrons and the volume of their collisional interaction with the neutral xenon is not enough to produce a significant increase in the plasma density.

These conclusions agree with the observational data presented and make it possible to explain them. Unfortunately, the absence of the data on the low-frequency (lower hybrid) wave activity in the spectra of the energetic electrons makes it impossible to present a complete picture of the event and draw final conclusions.

---

## References


Alfvén, H., *On the Origin of the Solar System*, Oxford Univ. Press, New York, 1954.

Galeev, A. A., and I. C. Chabibrachmanov, The critical ionization phenomenon in astrophysics, in *Proceedings of the Joint Varenna-Abastumani International School and Workshop on Plasma Astrophysics, May 1986, ESA-SP-251,* pp. 129-136, Eur. Space Agency, Paris, 1986.

Haerendel, G., Alfvén's critical velocity effect tested in space, *Z. Naturforsch., 37a*, 728, 1982.

Haerendel, G., M. C. Kelley, and R. F. Pfaff, Electric field measurements during the Condor critical velocity experiment, *J. Geophys. Res., 91* (A9), 9939, 1986.

Lizunov, G. V., V. N. Oraevsky, and A. S. Volokitin, Whistler generation by an ion beam limited in the transverse direction, *Plasma Phys. Rep., 21* (1), 85, 1995.

Marshall, J. A., J. L. Burch, E. Y. Chouieri, and N. Kawashima, CIV experiment on ATLAS 1,

*Geophys. Res. Lett., 20* (6), 499, 1993.

Mikhailovskii, A. B., *Theory of Plasma Instabilities*, Consult. Bur., New York, 1974.

Papadopoulos, K., On the physics of the critical ionization velocity phenomena, in Advances in *Space Plasma Physics,* pp. 33-58, Plasma Phys. Coll., Trieste, Italy, 1985.

Torbert, R. B., Review of critical velocity experiments in the ionosphere, *Adv. Space Res., 10*, 47, 1990.

Wescott, E. M., et al., Star of Condor: A strontium critical velocity experiment, Peru, 1983, *J. Geopys. Res., 91*, 9923, 1986.

---